

Shell-model calculation for two-neutrino double beta decay of ^{48}Ca

Liang Zhao and B. Alex Brown

National Superconducting Cyclotron Laboratory and Department of Physics and Astronomy, Michigan State University, East Lansing, Michigan 48824

W. A. Richter

Physics Department, University of Stellenbosch, Stellenbosch 7600, South Africa

(Received 12 February 1990)

The $2\nu\beta\beta$ decay matrix element of ^{48}Ca has been studied in a large basis shell-model space. The theoretical and experimental β^- and β^+ spectra and their relation to $2\nu\beta\beta$ are discussed. A new empirical effective interaction is found to give the best agreement to β^- and β^+ spectra with the effective Gamow-Teller operator $\bar{\sigma}t=0.77\sigma t$. The predicted $T_{1/2}=1.9\times 10^{19}$ yr differs by a factor of 2 from the present experimental limit of $T_{1/2}>3.6\times 10^{19}$ yr. We also compare the matrix elements obtained at various levels of the truncation in the shell-model space.

Double beta ($\beta\beta$) decay is a rare transition between two nuclei of the same mass number having a change of two units of nuclear charge. In cases of interest, ordinary single beta decay is forbidden because of the energy conservation or angular momentum mismatch. There are two modes of double beta decay. One involving the emission of two antineutrinos and two electrons (2ν mode), occurs in second order of the standard weak interaction theory and is independent of a possible small neutrino mass. The other involving no neutrinos and two electrons (0ν mode) violates the lepton number conservation and requires the neutrino to have a nonzero mass.^{1-3,7} Analysis of the experimental result to determine the character of the neutrino in $\beta\beta$ decay strongly depends on the precise calculation of the nuclear matrix elements. In particular, agreement between experiment and theory for the standard 2ν mode is one of the prerequisites for a reliable interpretation of the more exotic 0ν mode. In this paper, we study the $2\nu\beta\beta$ decay of ^{48}Ca which has the largest double beta decay Q value of any nucleus.

There are several difficulties with previous shell-model calculations for the $2\nu\beta\beta$ decay of ^{48}Ca . In cases where intermediate states in ^{48}Sc were considered explicitly the fp shell-model space was highly truncated,⁴⁻⁷ in other cases where the truncation was less severe the intermediate states were not calculated and the closure approximation was used instead.^{1,7,8} Also the effective interactions used were not always well tested with regard to the nuclear spectra. In a more recent calculation (Ref. 9) a new method was used to implicitly take into account the spectrum of the intermediate 1^+ states exactly. However, we will emphasize below the importance of testing the interactions with respect to the explicit intermediate spectrum.

The quasiparticle random phase approximation (QRPA) is another widely used method to calculate β and $\beta\beta$ decay matrix elements.¹⁰⁻¹² But there are many shortcomings with the QRPA. The equations violate the particle number conservation, and some approximations must be made to match the excited states of odd-odd nu-

clei based on the different initial and final even-even nuclei ground states. There are also uncertainties in the interactions used, and the QRPA equations become unstable with the interaction strengths just above realistic values.

In this paper, we calculate the nuclear matrix elements for $2\nu\beta\beta$ decay of ^{48}Ca and the related β^- and β^+ decay in the $0f_{7/2}, 1p_{3/2}, 0f_{5/2}, 1p_{1/2}(fp)$ shell-model space with a much larger basis than previously used and with a new and more reliable effective interaction. The truncation in the fp shell is defined by the set of partitions $f_{7/2}^{8-n}(p_{3/2}f_{5/2}p_{1/2})^n$. In this work, the partitions assumed for $^{48}\text{Ca}(0^+, T=4)$, $^{48}\text{Sc}(1^+, T=3)$, and $^{48}\text{Ti}(0^+, T=2)$ are ($n\leq 4$), ($n\leq 5$), and ($n\leq 4$), respectively. The $n\leq n_{\max}$ means that $n=0, \dots, n_{\max}$ are allowed. The corresponding J -scheme dimensions are 133, 5599, and 3613, respectively. This is an order of magnitude larger basis than has been used in previous calculations. Our calculations were carried out with the shell-model code OXBASH (Ref. 13) on a VAX computer. The most complete fp shell calculation should be based on the full-basis space ($n\leq 8$), but at present this is impossible because of the large dimensions involved. For example, the J -scheme dimension for the ^{48}Ti ground state is 10872 in the full-basis space. It is at the edge of our current computer capability. In later discussions, we will argue that our truncation is a good approximation to the full-basis space.

The model space for the intermediate nucleus (^{48}Sc) should include all states reachable by a one-body operator from the initial and final nuclei. Thus for our initial (^{48}Ca) and final (^{48}Ti) states which have $n\leq 4$, we include $n\leq 5$ configurations in the intermediate system. Then the $B(\text{GT})$ (where GT denotes Gamow-Teller) from the ^{48}Ti or ^{48}Ca ground states satisfy the sum rule,

$$\sum B(\text{GT}^-) - \sum B(\text{GT}^+) = 3(N - Z), \quad (1)$$

where

$$B(\text{GT}) = (\langle f | \sigma t | i \rangle)^2 = (\langle f | \|\sigma t\| | i \rangle)^2 / (2J_i + 1).$$

The effective interactions used in this paper are called MH (Muto and Horie¹⁴) and MSOBEP.¹⁵ The MH interaction has a long history. McGrory *et al.*¹⁶ started with the renormalized Kuo-Brown interaction¹⁷ and changed several $T=1$ two-body matrix elements (TBME), which involved the $f_{7/2}$ and/or $p_{3/2}$ orbits. Later McGrory *et al.*¹⁸ added 50 keV to the $f_{7/2}$ - $f_{5/2}$ diagonal $J=1$ TBME and introduced new single-particle energies. Based on Ref. 18, Muto and Horie¹⁴ shifted the monopole of the intershell matrix elements $\langle f_{7/2}j | V | f_{7/2}j \rangle^{T=0,J}$ ($j=p_{3/2}, p_{1/2}$, and $f_{7/2}$) by -0.3 MeV.

MSOBEP is a new effective interaction based on a modified surface (MS) one-boson exchange potential (OBEP).¹⁹ *Modified* refers to the addition of monopole (infinitely long range) terms to the central part of the potential, and *surface* refers to an assumed density dependence which empirically is surface peaked. This MSOBEP potential has been successful in reproducing the sd -shell energy levels in terms of a few parameters associated with the strengths of the various OBEP channels. Richter *et al.*¹⁵ have recently refit the parameters of this potential to 61 energy level data in the lower part of the fp shell, and this is the new interaction which we employ in the present work.

Based on previous beta decay and (p,n) reaction studies,²⁰ we use the effective Gamow-Teller operator

$$\tilde{\sigma} = \frac{g_A^{\text{eff}}}{g_A} \sigma = 0.77\sigma. \quad (2)$$

This is used because experimental $B(\text{GT})$ strengths are uniformly 30~50% less than the shell-model calculations. The missing strength can be explained by a combination of the coupling to Δ -particle- N -hole configurations,²¹⁻²⁵ and to the admixtures of 2p-2h configurations.²³⁻²⁵

For purposes of discussion, we introduce the matrix element for the $2\nu\beta\beta$ decay,

$$M_{\text{GT}}(E_m) = \sum_{m=1}^{E_m} M_{\text{GT}}^m(E_m) = \sum_{m=1}^{E_m} \frac{\langle 0_f^+ | \tilde{\sigma} t^- | 1_m^+ \rangle \langle 1_m^+ | \tilde{\sigma} t^- | 0_i^+ \rangle}{E_m + E_0}, \quad (3)$$

which is a function of the 1^+ excitation energy E_m in ^{48}Sc . $E_0 = T_0/2 + \Delta M$, where T_0 is the Q value for $\beta\beta$ decay of ^{48}Ca and ΔM is the mass difference between ^{48}Sc and ^{48}Ca , $T_0 = 4.27$ MeV and $\Delta M = -0.277$ MeV (Ref. 26). The total matrix element for $2\nu\beta\beta$ is given by $M_{\text{GT}}^{2\nu} = M_{\text{GT}}(E_m = \infty)$. The Fermi transition contribution vanishes when isospin is conserved. An estimate of its contribution with isospin-mixed wave functions indicates that it is small and can be neglected.⁵ The half-life is given by

$$\frac{1}{T_{1/2}} = G |M_{\text{GT}}^{2\nu}|^2, \quad (4)$$

where G is related to fundamental constants and the phase space integral.³ In fact, G depends somewhat on the GT strength distribution^{3,4} as well. Since the

strength distribution of Ref. 4 is close to ours, we use a value of $G = 1.10 \times 10^{-17} \text{ yr}^{-1} (\text{MeV})^2$ deduced from the first row in Table I of Ref. 4.

The closure approximation employed in the earlier calculations is defined by

$$B(\text{cls}) = \sum_m \langle 0_f^+ | \tilde{\sigma} t^- | 1_m^+ \rangle \langle 1_m^+ | \tilde{\sigma} t^- | 0_i^+ \rangle = \sum_{m,n} \langle 0_f^+ | \tilde{\sigma}_m \cdot \tilde{\sigma}_n t_m^- t_n^- | 0_i^+ \rangle \quad (5)$$

and

$$M_{\text{GT}}^{2\nu}(\text{cls}) = \frac{B(\text{cls})}{\langle E_m \rangle + E_0}. \quad (6)$$

In this approximation, $B(\text{cls})$ does not depend on the intermediate states. Estimates for the average energy $\langle E_m \rangle$ of the 1^+ states in ^{48}Sc were made to obtain $M_{\text{GT}}^{2\nu}(\text{cls})$.¹ These previous estimates can be compared with exact results, given by the comparison between $M_{\text{GT}}^{2\nu}$ and $M_{\text{GT}}^{2\nu}(\text{cls})$

$$\langle E_m \rangle = \frac{B(\text{cls})}{M_{\text{GT}}} - E_0. \quad (7)$$

The calculated matrix elements $M_{\text{GT}}(E_m)$ as a function of E_m for the MH and MSOBEP interactions are shown in Fig. 1(a). There are about 300 eigenstates in each curve from 2.52~15 MeV. The $M_{\text{GT}}^m(E_m)$ become negligibly small after about 12 MeV even though there are still many 1^+ states (over 5000) above this energy in the calculation.

To understand the $\beta\beta$ matrix elements, we examine the β^- and β^+ spectra. The theoretical $B(\text{GT}^-)$ strengths

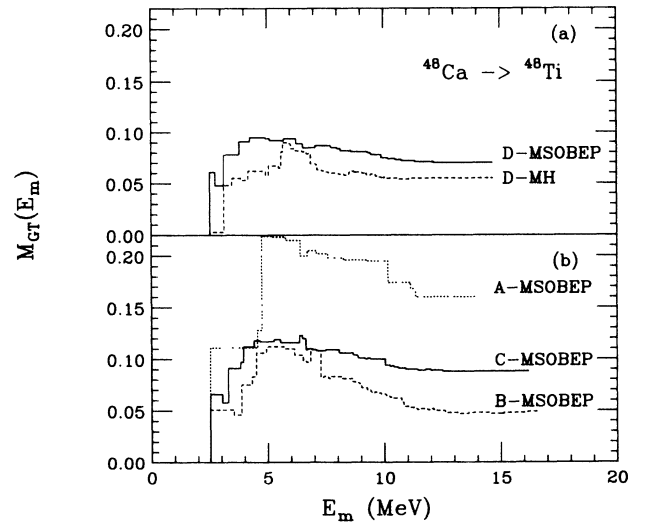


FIG. 1. $M_{\text{GT}}(E_m)$ as a function of E_m . The first $M_{\text{GT}}(E_m)$ is fixed at $E_1 = 2.52$ MeV. In (a), the solid line is obtained from the MSOBEP interaction, and dashed line from the MH interaction. The truncation for both curves is (D : $n \leq 4$ for ^{48}Ca and ^{48}Ti , $n \leq 5$ for ^{48}Sc). (b) shows the results for the MSOBEP interaction at different levels of truncation for (^{48}Ca , ^{48}Sc , ^{48}Ti): A ($n=0, n \leq 1, n=0$), B ($n \leq 1, n \leq 2, n \leq 1$), and C ($n \leq 2, n \leq 3, n \leq 2$).

versus E_m are shown in Fig. 2. The experimental distribution in Fig. 2(c) represents the strength above the background line in Fig. 1 of Ref. 28. There is additional strength in the background between 4.5 and 14.5 MeV not shown in Fig. 2(c) but indicated in the numerical comparisons made in Table I. There may be more strength in the background above 14.5 MeV which we will comment on later. The experimental spectrum in Fig. 2(c) was obtained by fitting the experimental cross section to a series of Gaussian peaks and then converting the cross section in each peak into a Gamow-Teller strength (Ref. 28 and B.D. Anderson, private communication). Because the experimental measurement has a finite resolution, the theoretical $B(GT^-)$ spectra are smoothed by a Gaussian. The $B(GT^-)$ spectrum with a high resolution (FWHM=100 keV) is shown in Fig. 2(a) for the MSOBEP interaction. The low resolution spectra for the MSOBEP (solid line) and MH (dashed line) interactions shown in Fig. 2(b) was obtained with FWHM=400 keV. One normalized factor is introduced in Fig. 2 to make the areas proportional to the $B(GT^-)$ strength. The $B(GT^-)$ values extracted from the (p,n) data are compared with the theory in Table I. For the broad peak between 4.5~14.5 MeV, the minimum experimental value of 8.61 corresponds to the spectrum in Fig. 2(c). An additional amount of 2.86 was estimated to be in the background not shown in Fig. 2(c).²⁸

The theoretical and experimental shapes are qualitatively the same as well as the $B(GT^-)$ strength values

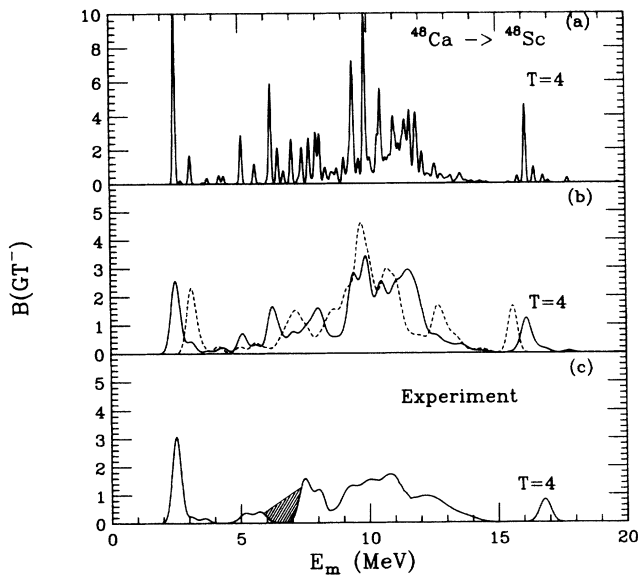


FIG. 2. The $B(GT^-)$ spectra for $^{48}\text{Ca} \rightarrow ^{48}\text{Sc}$. The high resolution spectrum (100 keV) obtained with the MSOBEP interaction is shown in 2(a). The low resolution spectra (400 keV) obtained with the MSOBEP (solid line) and MH interaction (dashed line) are shown in 2(b). The effective operator defined in Eq. (2) is employed in our calculations. The experimental $B(GT^-)$ from Ref. 28 and B.D. Anderson (private communication) is presented in 2(c). The hatched area indicates the uncertainty resulting from subtracting the Fermi strength in the $0^+(T=4)$ state at 6.8 MeV.

themselves (see Table I). But quantitatively there are some interesting differences which indicate a preference for the MSOBEP over the MH interaction. In the pure $j-j$ coupling model, the first 1^+ excited state in ^{48}Sc can be understood as a $(\pi f_{7/2} \nu f_{7/2}^{-1})$ particle-hole configuration. The theoretical calculation based on the MSOBEP interaction and the experimental data are both in good agreement with this simple picture. But for the MH interaction, this particle-hole state is the second 1^+ excited state located at 3.13 MeV. The first 1^+ of ^{48}Sc in the MH calculation has a negligibly small $B(GT^-)$ value. This state, however, has a relatively large overlap with ^{46}Ca plus a deuteron-cluster configuration, which explains why the state comes low in energy.

The total $B(GT^-)$ strengths in $T=4$ states are 0.78 and 0.77 for the MSOBEP and MH interactions, respectively. For the MSOBEP interaction, only $B(GT^-)=0.42$ is contributed by the single state at 16.1 MeV, the rest is spread between 15~20 MeV [see Fig. 2(a)]. But for the MH interaction, most of the $B(GT^-)$ strength (0.72) is in a single state at 15.4 MeV. Thus comparison with experiment again favors the MSOBEP interaction (see Table I).

The β^+ strength distribution and total strengths for theory and experiment²⁹ are compared in Fig. 3 and in Table I. There is the possibility of $B(GT^+)$ strength above 6 MeV in the data²⁹ not shown in Fig. 3. We see that the β^+ spectrum and $\sum B(GT^+)$ are strongly dependent on the effective interactions. The spectrum for the MSOBEP interaction is in best agreement with the experiment, especially for the first state (see Table I).

The calculated $M_{GT}^{2\nu}$ values are presented in Table II, and compared with previous calculations. We have modified the results from previous calculations to take into account the effective operator of Eq. (2). We note that the value of $\langle E_m \rangle = 5.86$ MeV assumed by Haxton is too large, in agreement with the conclusion of Ref. 4. We also note the excellent agreement between our result with the MH interaction and the result obtained with the new method of Ogawa and Horie⁹ who also used the MH

TABLE I. Summary of the $B(GT^-)$ and $B(GT^+)$ values obtained in the experiments and compared to the theoretical calculations with the MSOBEP and the MH interactions. An asterisk denotes a value unknown.

	E_m (MeV)	Experiment ^a	MSOBEP	MH
β^-	2.52-3.5	1.30	1.32	1.24
	3.5-14.5	8.61+2.86 ^b	12.31	12.39
	16.8 ($T=4$)	0.45	0.42 (0.62) ^c	0.72 (0.73) ^c
β^-	2.52	0.07	0.07	0.15
	3.0-6.0	0.49	0.50	0.51
	> 6.0	*	0.03	0.10

^aThe experimental $B(GT^-)$ and $B(GT^+)$ strengths from Refs. 28 and 29.

^bThe $B(GT)$ in the experimental background in the region of $4.5 \leq E_m \leq 14.5$ MeV (Ref. 28)

^cThe first number is the strength in the single strongest $T=4$ state, whereas the number in the bracket includes the additional strength from small states ± 500 keV on either side of the strongest state.

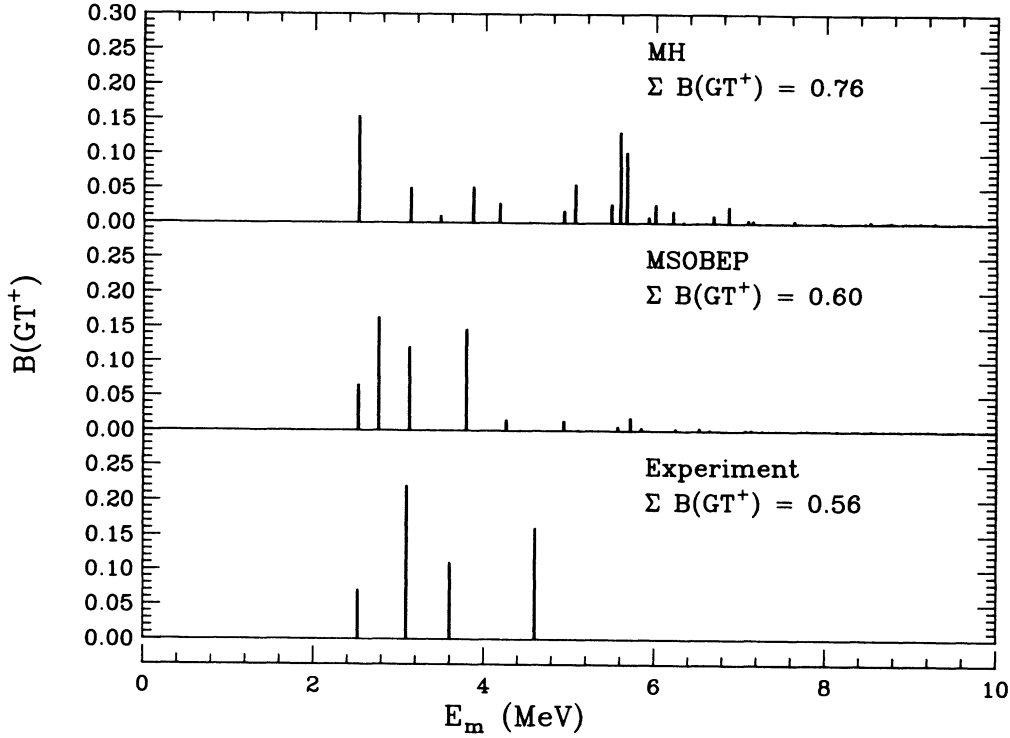


FIG. 3. The $B(GT^+)$ values for $^{48}\text{Ti} \rightarrow ^{48}\text{Sc}$. The experimental values from Ref. 29 are compared to the results obtained with the MSOBEP and MH interactions. The effective operator defined in Eq. (2) is employed in our calculations.

interaction. This new method implicitly takes into account the spectrum of intermediate states exactly in the full basis. But it does not produce the explicit intermediate state spectrum which was important for the β^- and β^+ comparisons made above. Also we note that the results obtained with the MSOBEP and MH interactions are not very different, indicating the relative stability of the calculation with respect to reasonable variations in the interaction.

There are several reasons why $M_{GT}^{2\nu}$ in the $2\nu\beta\beta$ decay of ^{48}Ca is relatively small. The energy region of the strongest $B(GT^-)$ strength (6~10 MeV) is mismatched from the region of the strongest $B(GT^+)$ strength (2.52~6 MeV). Also there is a systematic cancellation between the M_{GT}^m in the low and the high energy part (see

Fig. 1). The qualitative reason for this behavior can be understood as follows. In the simple j - j coupling model where the initial and final states are pure $f_{7/2}$ configurations, the only partitions for the intermediate 1^+ states which can be reached by β^- and β^+ transition are $A(\pi f_{7/2}\nu f_{7/2}^{-1})$, $B(\pi f_{5/2}\nu f_{7/2}^{-1})$, and $C(\pi f_{7/2}\nu f_{5/2}\nu f_{7/2}^{-2})$. β^- transitions can go to A or B and β^+ transitions can go to A or C . Thus the $\beta\beta$ transition can only go through A . These partitions will be mixed in the physical system, and in particular mixing of B and C will lead to two states $|1_1^+\rangle = \alpha|B\rangle + \beta|C\rangle$ and $|1_2^+\rangle = \beta|B\rangle - \alpha|C\rangle$, which can both be reached by β^- and β^+ transitions. The numerator of the $\beta\beta$ matrix element will then have the form

TABLE II. Comparison of the nuclear matrix elements $B(\text{cls})$ and $M_{GT}^{2\nu}$, the average excited energy $\langle E_m \rangle$ and half-life $T_{1/2}$. The shell-model space configurations are described by $f_{7/2}^{8-n}(p_{3/2}f_{5/2}p_{1/2})^n$ with $n=0$ to n_{max} for the fp shell referring to the initial (i), intermediate (m) and final (f) states.

Reference	Interaction	i	n_{max} m	f	$B(\text{cls})$	$M_{GT}^{2\nu}$ (MeV) ⁻¹	$\langle E_m \rangle$ (MeV)	$T_{1/2}$ (10 ¹⁹ yr)
Expt. (Ref. 27)								> 3.6
Present	MSOBEP	4	5	4	0.204	0.070	1.06	1.9
Present	MH	4	5	4	0.213	0.055	2.01	3.0
Ref. 9 ^a	MH	8	8	8		0.053		3.3
Ref. 1 ^a	KB (Ref. 1)	8		4	0.266			7.2 ^b (1.1 ^c)
Ref. 4 ^a	MH	2	2	2	0.278	0.073	1.94	1.7
Ref. 8 ^a	MBZ (Ref. 8)	0		0	0.216			
Ref. 6 ^a	KB (Ref. 17)	0		0	0.150			

^aModified by taking into account the effective operator in Eq. (2).

^bBased on an assumed $\langle E_m \rangle = 5.86$ MeV.

^cBased on the exact $\langle E_m \rangle = 1.06$ MeV.

$$\begin{aligned} & \langle 0_f^+ \| \sigma t^- \| 1_1^+ \rangle \langle 1_1^+ \| \sigma t^- \| 0_i^+ \rangle + \langle 0_f^+ \| \sigma t^- \| 1_2^+ \rangle \langle 1_2^+ \| \sigma t^- \| 0_i^+ \rangle \\ & = \alpha \beta \langle 0_f^+ \| \sigma t^- \| C \rangle \langle B \| \sigma t^- \| 0_i^+ \rangle - \alpha \beta \langle 0_f^+ \| \sigma t^- \| C \rangle \langle B \| \sigma t^- \| 0_i^+ \rangle . \end{aligned}$$

Thus we find two $\beta\beta$ routes each of which is nonzero but differing in sign so that they cancel. Mixing of B and C into A is important in modifying the $\beta\beta$ strength through the lowest 1^+ state relative to pure j - j coupling. This aspect of the $\beta\beta$ strength function shows up qualitatively in all of our calculations (see Fig. 1). And it is remarkable in our most complete calculations with the MSOBEP interaction that the total $M_{GT}^{2\nu}$ matrix element (0.070) is nearly exactly equal to the contribution from the first state alone (0.061).

We give the $B(GT^-)$, $B(GT^+)$, and M_{GT}^m values for the first ten eigenstates in Table III obtained with the MSOBEP interaction. They are the main positive contributions to $M_{GT}^{2\nu}$. The states with small $B(GT^-)$ and $B(GT^+)$ strengths will be missed in the experiment because of the finite resolution. Consequently some states will be seen in (p, n) and not (n, p) and vice versa. Nevertheless, the results given in Table III are in excellent agreement with the analysis of Ref. 29 based entirely on experimental data.

To study the effects of truncation, we now discuss the several cases of interest shown in Table IV. The $M_{GT}^{2\nu}$ for ^{48}Ca in more highly truncated fp -shell space are presented, where only the MSOBEP interaction is used. One of them is obtained from the truncation ($n_{\max}=2$) for ^{48}Ca , ^{48}Sc , and ^{48}Ti used by Tsuboi *et al.* with the MH interaction. (We note that at this level of truncation the MH interaction gives the lowest 1^+ state with a structure as expected in the simple picture discussed above.) The $B(GT)$ strengths from this space will not give the sum rule [Eq. (1)] because the intermediate state is incomplete. However, the $M_{GT}^{2\nu}$ is changed very little when $n_{\max}=3$ is allowed for ^{48}Sc . This indicates that the sum rule violation is not so important for $M_{GT}^{2\nu}$. From Table IV, we find that the $M_{GT}^{2\nu}$ in the highly truncated spaces differ significantly from the one in our expanded basis. The $M_{GT}(E_m)$ spectra in Fig. 1(b) show these differences in

detail.

To test the accuracy of our truncation, we compare the calculations for $M_{GT}^{2\nu}$ values in the space we used and in the full basis for ^{22}O in the sd shell and ^{46}Ca in the fp shell. These comparisons indicate that the truncation we used is a good approximation to the full space results. We may expect that the present $M_{GT}^{2\nu}$ value of ^{48}Ca will be reduced a further 5~10% if the full basis in the fp shell is employed. (Compared with these more complete calculations, a previous estimate⁵ of the extrapolation from the $n_{\max}=2$ space to the full-space value for $M_{GT}^{2\nu}$ is found to be in error by about a factor of 2.)

Beyond the fp shell-model space there are several processes that we should consider. The role of Δ -isobar admixtures have been investigated in previous work.^{21,22,24,25} The contribution from the direct excitation of the Δ -isobar nucleon-hole configuration, for which the excitation energy is about 300 MeV, is negligible^{8,10} because of the cancellation between β^+ and β^- and because of the large energy denominator in Eq. (3). The Δ -isobar admixtures in the low-lying states are already approximately taken into account in our calculation in the effective operator $\tilde{\sigma}t$ of Eq. (2) as well as in the effective interaction. In addition, 2p-2h admixtures beyond the fp shell can lead to $B(GT)$ strength at higher excitation.²³ The possible strength seen experimentally in the background above 6 MeV in β^+ and 15 MeV in β^- may be due to these 2p-2h admixtures. The effect of these 2p-2h admixtures in the low-lying states are also approximately taken into account in the effective operator and effective interaction. The contribution from the direct excitation of the 2p-2h configurations may again be small because of cancellation and large energy denominator, but should be investigated further.

In summary, we have studied the $2\nu\beta\beta$ decay of ^{48}Ca in a large basis shell-model space. An effective Gamow-Teller operator $\tilde{\sigma}t$ is employed, which describes $B(GT^-)$

TABLE III. The first ten $B(GT^-)$, $B(GT^+)$, and M_{GT}^m values obtained with the MSOBEP interaction.

E_m	$(\langle 1_m^+ \ \tilde{\sigma}t^- \ 0_i^+ \rangle)^2$	$(\langle 1_m^+ \ \tilde{\sigma}t^+ \ 0_f^+ \rangle)^2$	$\frac{\langle 0_f^+ \ \tilde{\sigma}t^- \ 1_m^+ \rangle \langle 1_m^+ \ \tilde{\sigma}t^- \ 0_i^+ \rangle}{E_m + E_0}$
2.520	1.102	0.065	0.061
2.759	0.022	0.163	-0.013
3.122	0.180	0.120	0.030
3.620	0.010	0.000	0.000
3.789	0.037	0.146	0.013
4.257	0.053	0.015	0.005
4.425	0.048	0.000	0.000
4.934	0.002	0.014	-0.001
5.104	0.305	0.001	-0.002
5.568	0.006	0.006	0.001

TABLE IV. Comparison of $M_{GT}^{2\nu}$ in different truncations. The shell-model space configurations are described by $f_{7/2}^{8-n}(p_{3/2}f_{5/2}p_{1/2})^n$ for the fp shell and $d_{5/2}^{6-n}(s_{1/2}d_{3/2})^n$ for the sd shell referring to the initial (i), intermediate (m) and final (f) states with $n=0$ to n_{\max} . The full-basis means $n_{\max}=8$ in the fp shell or $n_{\max}=6$ in the sd shell. The MSOBEP interaction was used for ^{48}Ca and ^{46}Ca and the interaction of Wildenthal (Ref. 20) was used for ^{22}O .

	i	n_{\max} m	f	$M_{GT}^{2\nu}$
$^{48}\text{Ca} \rightarrow ^{48}\text{Ti}$	0	0	0	0.124
	0	1	0	0.143
	1	2	1	0.049
	2	2	2	0.086
	2	3	2	0.088
	4	5	4	0.070
$^{46}\text{Ca} \rightarrow ^{46}\text{Ti}$	4	5	4	0.134
	Full	Full	Full	0.127
$^{22}\text{O} \rightarrow ^{22}\text{Ne}$	2	2	2	0.077
	4	5	4	0.041
	Full	Full	Full	0.039

and $B(\text{GT}^+)$ behavior well in the energy region (2.5~15.0 MeV). Of the two effective interactions we have employed, the new MSOBEP interaction seems to be a better interaction for the β^- and β^+ spectra. With this interaction we predict the $2\nu\beta\beta$ decay matrix element of ^{48}Ca is $M_{GT}^{2\nu}=0.070$ giving a half-life $T_{1/2}=1.9 \times 10^{19}$ yr, which differs by nearly a factor of 2 from the experimental limit²⁷ of $T_{1/2} > 3.6 \times 10^{19}$ yr. We believe that the most important aspect of these calculations which cannot be directly tested by the (p,n) and (n,p) experiments is the amount of strength in the (n,p) β^+ spectrum above 5 MeV in excitation. This is because there is a large uncertainty in the amount of Gamow-Teller strength in the background above this energy. The Gamow-Teller strength in this region may be sensitive to further refinements in the effective interaction as well as to direct excitation of 2p-2h states, and should be studied further. In addition, we believe that it is important to confirm and improve upon the present experimental limit. We plan to use the wave functions of ^{48}Ca and ^{48}Ti based on the MSOBEP interaction to calculate the $0\nu\beta\beta$ decay matrix elements.

This work was supported by the National Science Foundation under Grant No. PHY-87-14432.

¹W. C. Haxton and G. J. Stephenson, Prog. Part. Nucl. Phys. **12**, 409 (1984).
²M. Doi, T. Kotani, and E. Takasugi, Prog. Theor. Phys. **83**, 1 (1985).
³K. Muto and H. V. Klapdor, in *Neutrinos*, edited by H. V. Klapdor (Springer-Verlag, Heidelberg, 1988).
⁴T. Tsuboi, K. Muto, and H. Horie, Phys. Lett. **143B**, 293 (1984).
⁵B. A. Brown, in *Nuclear Shell Models*, edited by M. Vallieres and B. H. Wildenthal (World Scientific, Singapore, 1985), p. 42.
⁶L. D. Skouras and J. D. Vergados, Phys. Rev. C **28**, 2122 (1983).
⁷J. D. Vergados, Phys. Rep. **133**, 1 (1986).
⁸L. Zamick and N. Auerbach, Phys. Rev. C **26**, 2185 (1982).
⁹K. Ogawa and H. Horie, in *Nuclear Weak Process and Nuclear Structure*, edited by M. Morita, H. Ejiri, H. Ohtsubo, and T. Sato (World Scientific, Singapore, 1989), p. 308.
¹⁰K. Grotz and H. V. Klapdor, Nucl. Phys. **A460**, 395 (1986).
¹¹P. Vogel and M. Zirnbaaur, Phys. Rev. Lett. **57**, 3148 (1986).
¹²O. Civitarese, A. Faessler, and T. Tomada, Phys. Lett. B **194**, 11 (1987).
¹³A. Etchegoyen, W. D. M. Rae, N. S. Godwin, W. A. Richter, C. H. Zimmerman, B. A. Brown, W. E. Ormand, and J. S.

Winfield, Michigan State University NSCL Report No. 524, 1985.
¹⁴K. Muto and H. Horie, Phys. Lett. **138B**, 9 (1984).
¹⁵W. A. Richter, R. E. Julies, and B. A. Brown, submitted to Nucl. Phys. A.
¹⁶J. B. McGrory, B. H. Wildenthal, and E. C. Halbert, Phys. Rev. C **2**, 186 (1970).
¹⁷T. T. S. Kuo and G. E. Brown, Nucl. Phys. **A114**, 241 (1968).
¹⁸J. B. McGrory and B. H. Wildenthal, Phys. Lett. **103B**, 173 (1981).
¹⁹B. A. Brown, W. A. Richter, R. E. Julies, and B. H. Wildenthal, Ann. Phys. (N.Y.) **182**, 191 (1988).
²⁰B. A. Brown and B. H. Wildenthal, Ann. Rev. Nucl. Part. Sci. **38**, 29 (1988).
²¹C. D. Goodman *et al.*, Phys. Lett. **107B**, 406 (1981).
²²A. Bohr and B. R. Mottelson, Phys. Lett. **100B**, 10 (1981).
²³G. F. Bertsch and I. Hamamoto, Phys. Rev. C **26**, 1323 (1982).
²⁴A. Arima, K. Shimizu, W. Bentz, and H. Hyuga, Adv. Nucl. Phys. **18**, 1 (1987).
²⁵I. S. Towner, Phys. Rep. **155**, 263 (1987).
²⁶A. H. Wapstra and G. Audi, Nucl. Phys. **A432**, 1 (1985).
²⁷R. K. Bardin *et al.*, Nucl. Phys. **A158**, 337 (1970).
²⁸B. D. Anderson *et al.*, Phys. Rev. C **31**, 1161 (1985).
²⁹W. P. Alford *et al.*, Nucl. Phys. A (to be published).